DOI: 10.1002/chem.200600972

Ordered Arrays of Organometallic Iridium Complexes with Long Alkyl Chains on Graphite

Joe Otsuki,*[a] Tsubasa Tokimoto,[a] Yuki Noda,[a] Tomohiro Yano,[a] Takeshi Hasegawa,[b] Xiaoming Chen,[c] and Yoshio Okamoto[c]

Abstract: Iridium(III) *fac*-tris(2-phenylpyridine) *fac*-[Ir(ppy)$_3$] complexes equipped with long alkyl chains were prepared to examine their capability to form organized arrays on the surface of highly oriented pyrolytic graphite (HOPG). The molecules form lamellar arrays at the 1-phenyloctane/HOPG interface. From the analysis of the STM images, it was concluded that the molecules align with alkyl chains being interdigitated. Similar lamellar arrays were also obtained at the air/HOPG interface upon drop-casting of toluene solutions. The lamellar structure at the molecular level leads to rectangular two-dimensional crystalline domains a few hundred nanometers long (nanoslips). Infrared external reflection spectroscopy suggested that the adsorbed alkyl chains adopt the *trans*-zigzag conformation in the nanoslip, although the orientations of the zigzag plane of the alkyl groups are mixed. Cyclic voltammetry indicates fast electron transfer between the adsorbed molecules and the substrate and significant intermolecular electronic interactions. It was found that annealing at high temperatures is an effective method to prepare ordered assemblies more than a few micrometer scale (microslips). The orientations of the nanoslips prepared from the racemic mixture exhibited an apparent 12-fold symmetry, while its optically active enantiomer resulted in more irregular domains with a six-fold symmetry, implying an important role of chirality on packing at the molecular level and on the orientation of the domains at larger scales. When drop-cast from more concentrated solutions than a few hundreds of micromolar, multilayers were obtained, in which the alkyl chains in the molecules are more or less perpendicular to the surface. This structure can be transformed into the nanoslips upon standing.

Keywords: iridium · nanostructures · physisorption · self-assembly · surface chemistry

Introduction

Organized molecular assemblies on surfaces would be a basis for the bottom-up construction of molecule-based materials and devices.[1] Especially, molecular layers comprising of electro- and photo-active compounds deserve special attention from the viewpoint of molecular electronic/photonic applications. Alkylated compounds have a high affinity for the surface of highly oriented pyrolytic graphite (HOPG), and many of them form organized monolayers at the solid/liquid interface, which can be imaged with scanning tunneling microscopy (STM) at molecular resolution under ambient conditions.[2] The adlayers of porphyrins and phthalocyanines with long alkyl chains have attracted intense attention with this respect.[3,4] Another important class of photo/electro-active compounds are trischelating octahedral metal complexes, wherein a d_6 metal ion (e.g., Ru^{2+}, Os^{2+}, and Ir^{3+}) is chelated by three bidentate ligands (e.g. 2,2′-bipyridine). In contrast to planar compounds represented by porphyrins and phthalocyanines, this type of complexes has rarely been adsorbed on HOPG.[5] In fact, an ordered array of an octahedral complex with alkyl chains on HOPG has never been reported to date, to the best of our knowledge, despite the fact that introducing alkyl chains is so powerful that a variety of alkylated molecules have been made into

[a] Prof. J. Otsuki, T. Tokimoto, Y. Noda, T. Yano
College of Science and Technology
Nihon University
1-8-14 Kanda Surugadai, Chiyoda-ku, Tokyo 101-8308 (Japan)
Fax: (+81) 3-3259-0817
E-mail: otsuki@chem.cst.nihon-u.ac.jp

[b] Prof. T. Hasegawa
Department of Chemistry
Graduate School of Science and Engineering
Tokyo Institute of Technology and PRESTO (Japan) Science and Technology Corporation (JST)
Meguro-ku, Tokyo 152-8551 (Japan)

[c] Dr. X. Chen, Prof. Y. Okamoto
EcoTopia Science Institute
Nagoya University
Furo-cho, Chikusa-ku, Nagoya 464-8603 (Japan)

arrays.[2] It is anticipated that an octahedral complex may be adsorbed on the HOPG surface if alkyl chains can be introduced at three positions that are in the facial relationship with each other. This is because the three facial points can touch a planar surface simultaneously as these are on the same side of the spherical complex. However, it is usually difficult to introduce substituents selectively into facial positions, since the reaction of ligands and a metal ion would usually end up in the formation of a mixture of meridional and facial isomers.

Iridium(III) *fac*-tris(2-phenylpyridinato-$N,C^{2'}$), *fac*-[Ir(ppy)$_3$], and its derivatives are potential candidates for highly efficient organic light emitting diodes.[6] The reaction of iridium precursors with 2-phenylpyridine yields predominantly *fac*-[Ir(ppy)$_3$] under high temperature conditions.[7] Hence, the introduction of alkyl groups to either the pyridine or phenyl ring at the *para*-position to the central metal ion allows us to obtain complexes having alkyl chains at the desired facial positions. We have prepared such complexes, **Ir-C$_n$** (n = 18, 22, 30), and investigated the molecular arrays spontaneously formed on HOPG. Here, we report for the first time a successful implementation of the long-alkyl-chain strategy for an octahedral metal complex, which consequently leads to organized two-dimensional assemblies of organometallic iridium complexes.

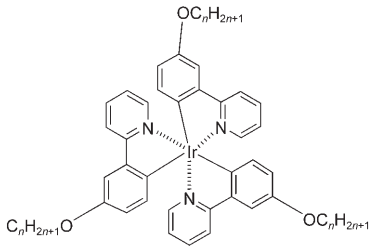

Ir-C$_n$ (n = 18, 22, 30)

Results and Discussion

Assemblies at the liquid/solid interface: Samples for STM observation at the liquid/solid interface were prepared by depositing a drop of a 1-phenyloctane solution of **Ir-C$_n$** on freshly cleaved HOPG via a syringe. Figure 1a shows an STM image obtained for a 1 mM solution of **Ir-C$_{18}$** on HOPG. The image shows several crystalline domains with dimensions of tens of nanometers. In each domain, a parallel line pattern is observed. The bright lines of different directions meet at domain boundaries. It is most likely that these lines correspond to the row of aligned Ir(ppy)$_3$ units, while the gaps are filled by alkyl chains. The separation between the neighboring lines is d_{18} = 3.5 nm. It has been found that the other **Ir-C$_n$** complexes also assemble themselves into similar parallel line patterns. The line separations for **Ir-C$_{22}$** and **Ir-C$_{30}$** were found to be 4.0 and 5.0 nm, respectively. These separations (d_n in nm) are plotted against the alkyl chain length (n) of **Ir-C$_n$** as in Figure 1b. The data are

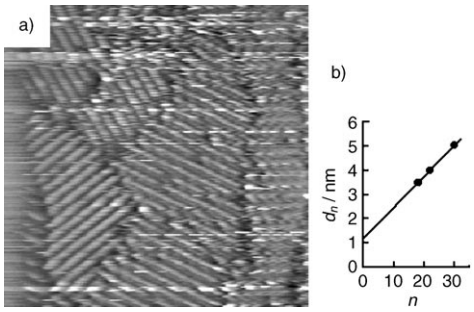

Figure 1. Arrangement of **Ir-C$_n$** at the 1-phenyloctane/HOPG interface. a) STM image of **Ir-C$_{18}$** (100×100 nm^2; I = 98 pA; V = −1.3 V). b) Dependence of the line separation (d_n) on the carbon number (n) in the alkyl chain.

fitted by a linear relationship with a correlation constant of 1.0: $d_n = 0.125 \times n + 1.25$.

The slope in the equation, 0.125 nm, matches well with the length per carbon atom along the axis of an alkyl chain extended on HOPG (0.128 nm).[2a] The intercept, 1.25 nm, is about the size of the Ir(ppy)$_3$ core on the basis of the crystal structure.[8] Hence, the STM image is consistent with a lamellar structure model, in which intervals are filled with extended alkyl chains oriented nearly perpendicular to the bright lines. An alkyl chain may be snugly fit into the gap made by a pair of alkyl chains of an **Ir-C$_n$** molecule, since the width per close packed alkyl chain is 0.4–0.5 nm[9] and the oxygen–oxygen distances on the periphery of the Ir(ppy)$_3$ core are about 1.0 nm. A possible arrangement of **Ir-C$_{18}$** on HOPG is depicted in Figure 2 on the basis of these

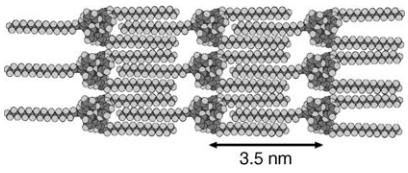

Figure 2. Possible arrangement of **Ir-C$_{18}$** on HOPG consistent with the STM images at the liquid/solid interface.

considerations. In this figure, the orientation of the alkyl-chain plane (all represented by the flat orientation) and the chirality of the Ir(ppy)$_3$ core (represented by the Λ enantiomer) are not taken into account. These aspects will be discussed for assemblies at the air/solid interface in later sections.

Despite repeated attempts, images for individual Ir(ppy)$_3$ units have not been obtained. This may probably be, at least partly, due to an intrinsic difficulty to obtain a high resolution image for samples with large undulations. Other factors which may be involved include a dense packing of the Ir(ppy)$_3$ core or some mobility of the molecules under the conditions of STM measurements.

Assemblies at the air/solid interface—observation with dynamic force microscopy (DFM): We have also prepared organized assemblies of **Ir-C_{18}** at the air/solid interface by a simple drop-cast method and investigated their morphology. In a typical sample preparation, a 4 μL solution of **Ir-C_{18}** in distilled toluene was dropped via a syringe on the surface of HOPG ($12\times12\,mm^2$), which was then air-dried. Thus prepared substrate was subjected to DFM observations. The observed images were relatively homogeneous over the whole substrate, although the density of the molecules somewhat depends on the macroscopic positions on the substrate. Therefore, the following discussion is based on the most widely observed morphologies for a given concentration of the cast solution.

Figure 3 displays the surface morphologies as observed with DFM. When the concentration of the cast solution is less than ≈100 μM, needlelike protrusions are found scattering around on the surface, as shown by the $5\times5\,\mu m^2$ image in Figure 3a. The needlelike objects are in fact nearly rectangular crystalline domains (nanoslips) with well-defined linear edges, with typical domain size being a few tens of nanometer wide and ≈200 nm long, as shown in the magnified image in Figure 3b. The cross section of the nanoslips shows that the height is homogeneous at 0.63 ± 0.11 nm. This apparent height measured by DFM indicates that the nanoslips have monolayer thickness. In fact, this height is between the height of the $Ir(ppy)_3$ core in the molecule, which is about 1 nm, and the thickness of an alkyl chain (0.5 nm). This indicates that the DFM, under the present measurement conditions, is less sensitive to the 1 nm high $Ir(ppy)_3$ unit. This is probably because the attractive force exerted by an isolated blip is largely cancelled by the reduced attractive force from the surrounding flat part of the molecules, as the tip is retracted when tracing above the blip.[10]

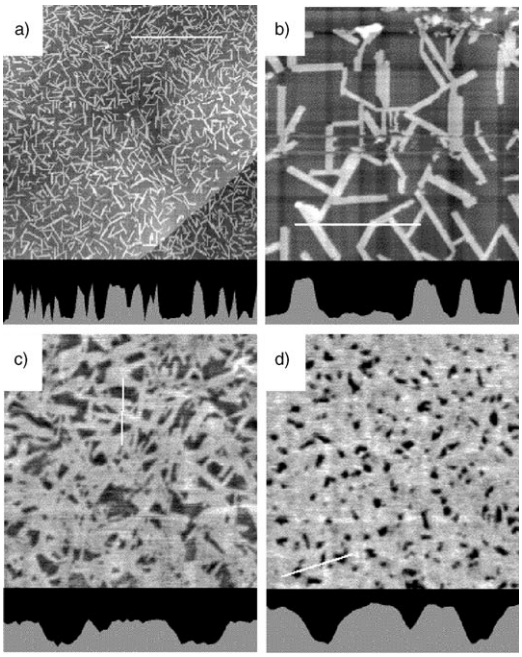

Figure 3. DFM images of the assemblies of **Ir-C_{18}** at the air/solid interface on HOPG prepared by drop-casting toluene solutions. The full scale in the height profiles is 1.5 nm. a) Prepared from a 25 μM solution; $5\times5\,\mu m^2$. b) Prepared from a 25 μM solution; $1\times1\,\mu m^2$. c) Prepared from a 100 μM solution; $1\times1\,\mu m^2$. d) Prepared from a 250 μM solution; $1\times1\,\mu m^2$.

The use of less concentrated cast solutions resulted in the appearance of similar nanoslips, only that the surface density was lower. In the surface assemblies prepared from more concentrated solutions, on the other hand, differently oriented nanoslips partly merge into a membranous layer. An example is shown in Figure 3c, which was prepared from a 100 μM cast solution. This trend is more highlighted by the image in Figure 3d, which was prepared from a more concentrated 250 μM solution. In this image most of the surface is covered by the monolayer film of **Ir-C_{18}**.

Observation with STM: The STM has revealed the inner structure of the nanoslips. Figure 4a shows that each nanoslip consists of a bundle of bright lines running along the long axis of the slip. The gap between the rows is 3.6 nm, which is identical with that observed for the array at the 1-phenyloctane/HOPG interface. This suggests that the molecular arrangement in the liquid/solid interface and in the air/solid interface is identical as shown in Figure 2. Thus, the bright lines most likely correspond to the rows of the aligned $Ir(ppy)_3$ units. The preferential growth directions in the case of liquid/solid and air/solid interfaces appear different, however; the domain grows more along the lines in the air/solid interface, whereas the domains tend to be wider in the direction perpendicular to the lines at the liquid/solid interface. Despite repeated attempts, we were not able to obtain a molecularly resolved STM image at the air/solid interface either, as can be seen from the narrower area scan in Figure 4b. More detailed analysis of the molecular arrangement in the nanoslips will be described in a later section in relation to the chirality of the molecule.

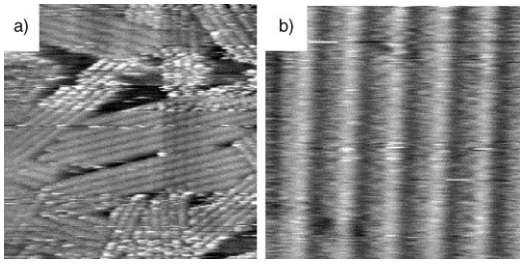

Figure 4. STM images of the two-dimensional nanoslips. a) Wide area image ($100\times100\,nm^2$; $I=3.0$ pA, $V=-1.1$ V). b) Close-up image ($20\times20\,nm^2$; $I=3.0$ pA, $V=-0.9$ V).

Infrared external-reflection spectroscopy (IR-ERS): The IR-ERS was employed to obtain information on the conformation of alkyl chains in the assembly at the air/solid interface. The measurements were performed with *p*-polarized IR ray with an angle of incidence of 50° from the surface normal. Figure 5 shows IR-ERS spectra in the C–H stretching vibra-

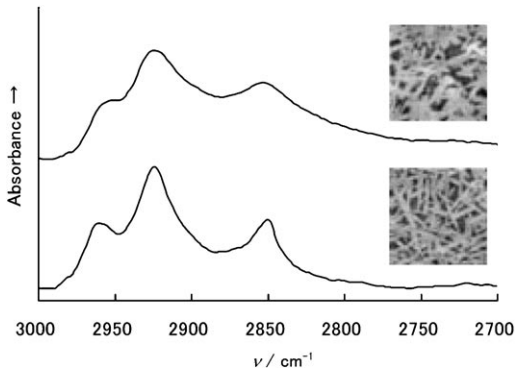

Figure 5. C–H stretch region in the infrared spectra for two different samples of nanoslips of **Ir-C$_{18}$** on HOPG. The upper spectrum is for a high density sample prepared from a 100 μM toluene solution, while the lower spectrum is for a low density sample from a 50 μM solution. Typical DFM morphologies (250×250 nm^2) for respective samples are shown in the insets.

tion region for the nanoslips on the surface with different densities. Typical surface morphologies of the IR samples are shown as the insets in the figure.

IR-ERS measured on a nonmetallic surface is known to have a unique surface selection rule that the surface parallel transition moment yields a negative absorbance band, whereas the surface normal one yields positive absorbance when the molecule has a specific orientation in the monolayer and the angle of incidence is less than Brewster's angle. Since the angle of incidence in this study (50°) is less than the Brewster's angle (ca. 60°) of the HOPG/organic layer interface, the surface selection rule would be held. In the spectra, however, all the bands appear positively, which does not obey the rule. This strongly suggests that the alkyl-chain planes have mixed rotation angles about the axis of the chain. Two energy-minimized orientations have been found for alkane molecules adsorbed on HOPG by molecular mechanics calculations.[9] In one orientation, the plane including the zigzag carbons is parallel to the basal plane of graphite, which is denoted as flat orientation. In the other orientation, the zigzag carbons are on a plane perpendicular to the surface, which is called vertical orientation. In the situation wherein these two orientations are mixed, the IR-ERS spectra should resemble normal IR transmission spectra.

Besides, peak maxima in the IR spectra provide information on the conformation of the alkyl chains. The lower density sample prepared from a 50 μM solution is covered with nanoslips that touch other nanoslips at the ends, as the DFM image shows in the inset. The symmetric methylene stretching vibration, $\nu_s(CH_2)$, band appears at 2850 cm^{-1}, which suggests that the alkyl chain has the all *trans*-zigzag conformation.[11] On the contrary, the asymmetric methylene stretching vibration, $\nu_a(CH_2)$, band is found at 2924 cm^{-1}, which suggests that the alkyl chain has *gauche*-rich conformations.[11] The band location of the $\nu_a(CH_2)$ band is, however, known to be influenced by the Fermi resonance band originated from the methylene scissoring band at 1466 cm^{-1}, which makes the band location inaccurate. Therefore, the $\nu_s(CH_2)$ band is more appropriate for the discussion, and we can conclude that the adsorbed molecules have highly ordered alkyl chains. Furthermore, the in-skeleton asymmetric methyl stretching vibration, $\nu_a(CH_3)$, band is found at 2960 cm^{-1}. This vibration is in parallel with the *trans*-zigzag plane of an alkyl chain, corroborating the all *trans*-zigzag conformation.

On the other hand, the nanoslips in the higher density sample prepared from a 100 μM solution are more in contact with others forming a partly membranous planar layer. The spectrum is broader, with the $\nu_s(CH_2)$ band shifted to 2853 cm^{-1}, higher than that for the lower density sample and the $\nu_a(CH_2)$ band appears at almost at the same position (2924 cm^{-1}). These spectral changes indicate that the alkyl chains in the denser sample with a membranous morphology contain *gauche*-rich conformations. Apparently, alkyl chains must bend to fill the gaps made by differently oriented nanoslips to form the planar membranous layer. This argument is consistent with the $\nu_a(CH_3)$ band shifts to 2952 cm^{-1}. This band location is assigned to the out-of-skeleton $\nu_a(CH_3)$ band, which evidences that the conformation has become disordered in concert with the inferior order of the alkyl chains.

Cyclic voltammetry: Cyclic voltammetry showed that **Ir-C$_{18}$** undergoes a reversible redox reaction at 0.20 V versus ferrocenium/ferrocene in a homogeneous acetonitrile/THF 1:2 solution, corresponding to the formal oxidation of the Ir^{3+} to Ir^{4+}.[12] Cyclic voltammetry was also performed for a drop-cast and dried sample on HOPG by placing an electrolyte solution on the substrate covered with the nanoslips to examine the electronic communication between the substrate and the molecules in the nanoslips. Figure 6 shows cyclic voltammograms measured in a 0.5 M aqueous Na_2SO_4 solution for an **Ir-C$_{18}$** sample prepared from a 5 μM cast solution. The scan rate was varied from 0.1 to 1 V s^{-1}. The peak current values, which are obtained by subtracting the charging current from the data, are in proportion to the scan rate

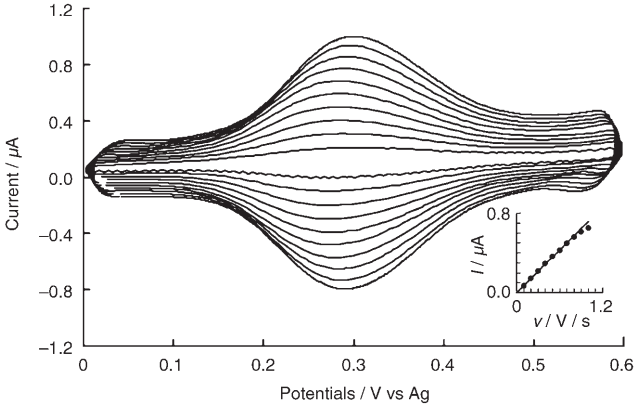

Figure 6. Cyclic voltammetry for **Ir-C$_{18}$** on HOPG. a) Scan rate dependent cyclic voltammograms (0.1–1 V s^{-1}). b) Relationship between the peak current values and scan rates.

as shown in the inset, which confirms that the reaction is due to the surface immobilized species. The anodic and cathodic peak potentials are identical, irrespective of the scan rate; this indicates that the electron transfer reaction between the molecules and the substrate is fast compared with the time scale of the experiment. Besides these ideal behaviors, the full width at half maximum is ≈ 160 mV, which is much larger than the value of 91 mV for noninteracting surface species. In principle, this can be due to surface inhomogeneity and/or interaction among redox active species. As judged from the images of DFM, and otherwise highly symmetrical voltammograms, it is likely that the electrochemical environment for the $Ir(ppy)_3$ unit is sufficiently homogeneous. Therefore, it can be deduced that there are significant electronic interactions among the $Ir(ppy)_3$ units, most likely along the molecular row.

Annealing effect: The nanoslips on HOPG at the air/solid interface are stable; no apparent morphology changes are noticed over weeks, as long as the sample is kept at room temperature. However, we have found that annealing at higher temperatures causes a large morphology change in the surface assembly. Figure 7a shows a DFM image for a

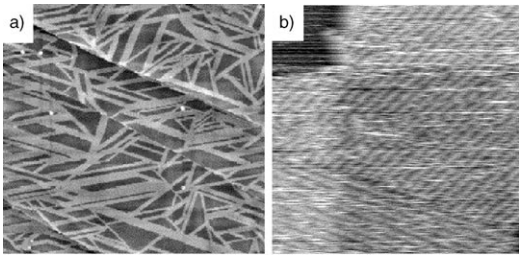

Figure 7. Samples of **Ir-C$_{18}$** on HOPG, annealed at 125 °C for 40 min. a) DFM image (5×5 μm^2). b) STM image (100×100 nm^2; $I=3$ pA; $V=-1.0$ V).

drop-cast sample, which was then annealed in an oven for 40 min at 125 °C, a temperature lower than the melting point of **Ir-C$_{18}$** (145 °C) by 20 °C. Annealing at temperatures around the melting point resulted in a similar morphology change. The nanoslips grow at the expense of other nanoslips, giving rise to a network of long slips of two-dimensional linear crystalline domains (microslips). The growth of the domain along the long axis stops when encountered with the side of another domain, but some domains extend over a few micrometers. The height of these microslips is identical to that of the nanoslips before annealing. The STM image in Figure 7b for one of these large area domains clearly shows that the bright lines are along the long axis of the microslip as is the case for nanoslips. The separation between the bright lines is also identical to that of nanoslips before annealing. Thus, the ordered domain can be obtained in a large area by annealing.

Orientation of the nanoslips and chirality: Upon drop-casting, the nanoslips are spread over a wide area on the surface, as exemplified by the image in Figure 3a. The 2D-Fast Fourier Transform (FFT) was employed to see if there are any preferred orientations or any correlation with the symmetry of the HOPG surface underneath. The FFT on the DFT image in Figure 3a is shown in Figure 8a, which indicates that the nanoslips are evenly distributed with a 12-fold angular symmetry, or in six different orientations. The orientations of the enlarged microslips on annealed samples also show the 12-fold symmetry. In general, alkanes and simple derivatives thereof adsorb on the HOPG surface with a six-fold symmetry, reflecting the underlying symmetry of graphite. The strong adsorption of alkane molecules on graphite surface is explained by the fortuitous match of the distance between the centers of the hexagons of the graphite lattice, 2.46 Å, and the distance between alternate methylene groups of the hydrocarbon backbone, 2.51 Å.[2a] Thus, the long axis of an alkyl chain is expected to orient parallel to one of the three directions of the lines connecting the centers of the hexagons, giving rise to a six-fold symmetry, or three different orientations. It may not be surprising, though, that six different orientations arise if the growth directions of the two-dimensional crystal are offset by an angle somewhere between 0 and 30° from one of the symmetry axes of the underlying graphite. To give the apparent 12-fold symmetry as in the present case, the offset angle must be $\approx 15°$.

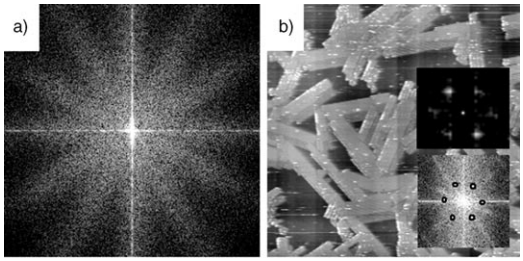

Figure 8. Orientations of racemic monolayer slips on HOPG. a) 2D-FFT of the DFM image in Figure 3a. Six orientations are discerned. b) STM image (500×500 nm^2; $I=3$ pA, $V=-1.05$ V). The lower inset shows the FFT of this image, superimposed with the FFT of the underlying HOPG, of which the original data are shown in the upper inset.

A model of the molecular arrangement on the graphite surface consistent with the above argument is presented in Figure 9. In the model, the long axis of the alkyl chains in a molecule is oriented in the direction commensurate with the graphite surface, along the x axis indicated in the figure. Then, the next molecule in the same row is placed slightly shifted from the eclipsed position in such a way that the growth direction of the crystal is offset by $\approx 15°$ from the y axis. There can be another equivalent orientation with the offset angle of about $-15°$, giving rise to a pair of nanoslips rotated by 30°, which are mutually mirror images. There are three equivalent directions rotated by 60° on the HOPG surface for this pair of mirror images, which accounts for the

total of six different orientations separated by 30°, as experimentally observed. Figure 8b shows an STM image and its 2D-FFT (lower inset) for an area of $500 \times 500\ nm^2$ containing nanoslips. The every 30° distribution is again clearly demonstrated, although only three orientations are present due to a limited number of nanoslips in the imaged area. The underlying graphite surface was also scanned by changing the tunneling conditions ($I = 30$ pA, $V = 0.03$ V) and the obtained image was treated with 2D-FFT, as shown in the upper inset. Comparison of these FFTs reveals that the nanoslip orientations and the symmetry axes of graphite are offset in the way consistent with the nanoslip orientations proposed in Figure 9, although the exact evaluation of the relevant angles is difficult due to experimental uncertainties.

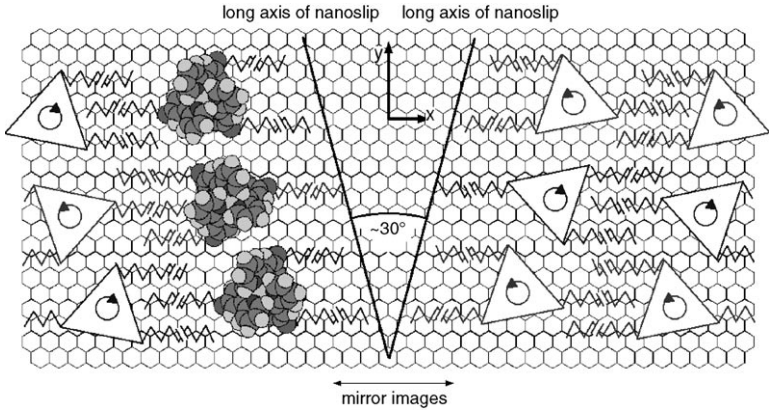

Figure 9. Schematic drawing of the proposed arrangement of molecules in a pair of mirror image nano- and microslips. There are other two sets of pairs rotated by 60 and 120° from this pair, accounting for the total of six different orientations. This drawing is not meant to represent the precise molecular arrangement but to illustrate the orientation with respect to the underlying graphite surface and the racemic nature of the nano- and microslips.

If the $Ir(ppy)_3$ unit joining three alkyl chains were achiral, the mirror image nanoslips would be isoenergetic with each other. However, the sample used here is a racemic mixture of the Δ and Λ enantiomers. Therefore, the chirality may play a role in the assembly process and the resulting two-dimensional structure.[2b,13] An especially relevant question is whether each nanoslip is a racemate, which contains both enantiomers, or a conglomerate, which comprises of only one of the enantiomers.

To shed light on this matter, we have isolated Δ- and Λ-**Ir-C$_{18}$** enantiomers (enantiomeric excess $> \approx 90\%$) by means of chiral column chromatography. Then the optically active material was drop-cast in the same way as for the racemic mixture. Here only the results obtained for the Δ isomer are presented, since both enantiomers gave the same results as expected. The monolayer domains scatter around on the surface as in the racemic mixture as can be seen in Figure 10a. However, the shapes of the domains are more irregular than those prepared from the racemic mixture, compare the image with that in Figure 3a. As for the orientation distribution, three different orientations are apparent from the 2D-FFT as shown in the inset, although the FFT image is significantly blurred reflecting the irregular shape of each domain. A DFM image for another area containing more extended domains is shown in Figure 10b. The shapes of the domains are again somewhat irregular as compared with racemic samples. The 2D-FFT shows more clearly three orientations rotated by 60° each other. This is in stark contrast to the racemic mixture, for which six different orientations are obtained. The different morphologies between the two-dimensional domains from racemic and optically active materials strongly suggest that their molecular arrangements in the domains are different.

Figure 10c shows a DFM image for an annealed sample of Δ-**Ir-C$_{18}$**. Straight edges oriented 60° to each other are recognized, in contrast to the 30° angle found for annealed samples of racemic mixture, see Figure 7a. In addition, there are many curved edges, which are not found in racemic samples. That the morphology of the optically active material is different from that of the racemic mixture also for annealed samples indicates that the difference in structure is not merely due to the kinetic effect, such as the rate of surface migration, but due to thermodynamics. Our attempts to obtain an STM image afforded only diffuse unclear images. We believe that this is due to a more disordered, and hence more mobile, molecular arrangement as im-

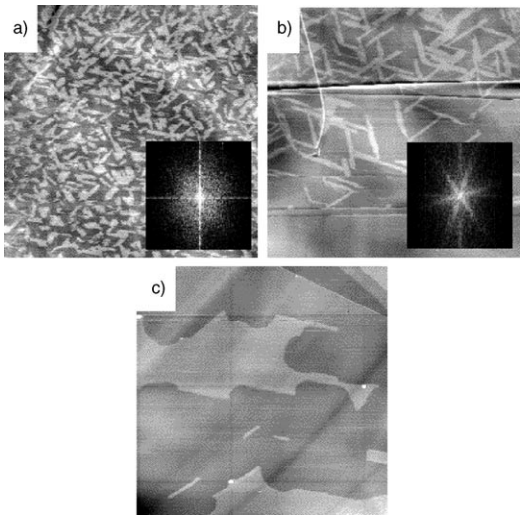

Figure 10. DFM images ($5 \times 5\ \mu m^2$) of monolayer assemblies of Δ-**Ir-C$_{18}$**. a) Image for an area with scattered molecular domains and its 2D-FFT. b) Image for another area with larger domains and its 2D-FFT for the upper part (above the crevice on the HOPG surface). c) Annealed (ca. 125 °C for 20 min) sample.

plied from the irregular shapes of the domains.

On the basis of the above observations, we have concluded that the molecular arrangement in the two-dimensional domains from the optically active **Ir-C$_{18}$** is different from that of racemic **Ir-C$_{18}$**. This in turn leads to the conclusion that the nano- and microslips prepared from the racemic mixture of **Ir-C$_{18}$** are racemates. This conclusion is incorporated in the schematic representation of a possible molecular arrangement in the nanoslips in Figure 9.

Multilayer assemblies: When (racemic) assemblies were prepared from solutions more concentrated than a few hundreds of micromolar, a different morphology was observed. Figure 11 shows a DFM image for a sample prepared by

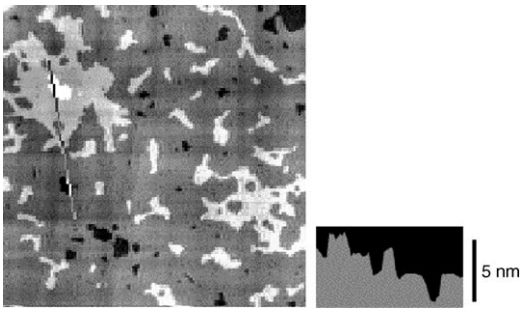

Figure 11. DFM image and a height profile for multilayers of **Ir-C$_{18}$** at the air/solid interface on HOPG ($2.5\times2.5\ \mu m^2$).

drop-casting a 1 mM toluene solution. Molecules are assembled to form a mosaic layered structure. The layers are extremely flat at the molecular level as the height profile shows. The thicknesses of the layers are integer multiples of a fundamental thickness of 2.6 ± 0.3 nm. It is unlikely that the molecules are lying flat as in the nano- or microslips, since the repeat unit of 2.6 nm could not be explained. Also, the structure of the layer seems not to be directed by the HOPG surface but to be intrinsic to the molecule, since the thickness of the first layer directly touching the substrate surface is the same as that of the second and third layers, which have no interaction with the surface. Thus, it is most likely that the layers consist of close packed molecules in a conformation with alkyl chains more or less perpendicular to the surface, since the length of the alkyl chain of 18 carbon atoms, 2.3 nm, is close to the measured thickness of the layer.

We have found a time evolution of the layered structure to form nanoslips. Figure 12a shows a case in which a single layer structure was observed on HOPG. The image was taken about 5 min after drop-casting. The height of amorphous-shaped plateaus is 2.5 nm, which is identical to that observed in the multilayer structure as discussed above. Therefore, we assume their structures are common, in which molecules are packed with the alkyl chains oriented upright. There are also features that appear like needles in the image, which are in fact the nanoslips. Upon standing at

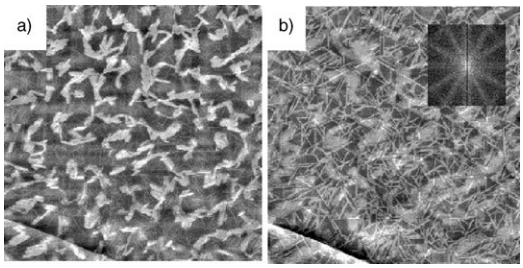

Figure 12. DFM images for a time evolution of **Ir-C$_{18}$** assemblies ($5\times5\ \mu m^2$). a) About 5 min after drop-casting. b) The same area an hour later. 2D-FFT is shown in the inset.

room temperature, more and more needles appeared gradually, as the DFM image in Figure 12b shows, which was taken an hour later for the same area. The 2D-FFT clearly shows the 12-fold symmetry for the newly emerged nanoslips. Thus, the layered structure transforms into the nanoslips, which is apparently more stable on the HOPG surface.[14]

Conclusions

In summary, we have shown that ordered arrays of iridium cyclometallated complexes can be prepared on HOPG both at the liquid/solid and air/solid interfaces. The key to the success was to introduce alkyl chains to the metal complex unit at the facial positions, which was made possible by the selective reactivity of the iridium phenylpyridine cyclometallation reaction.

The alkylated iridium complexes assemble into a lamellar structure on HOPG both at the liquid/solid and air/sold interfaces, in which the metal complex units align in rows. In the air/solid interface molecular assemblies, which were prepared by drop-casting toluene solutions of the racemic mixture, give rise to monolayer rectangular domains with the long axis parallel to the molecular rows (nanoslips). In the nanoslips, it was indicated by IR-ERS that the adsorbed alkyl chains adopt the *trans*-zigzag conformation but the vertical and flat orientations of the hydrocarbon plane are mixed. Cyclic voltammetry showed a fast electron transfer between the iridium complexes in the nanoslips and the HOPG substrate and a significant intercomplex electronic interaction. It was found that annealing the nanoslip sample at higher temperatures is a simple and powerful means to prepare larger two-dimensional single crystalline domains (microslips). The orientation of the nanoslips from the racemic mixture has a 12-fold angular symmetry, while that from optically active complexes has a six-fold symmetry. Thus, the chirality of molecules plays an important role in the packing of the molecules and the angular distribution of the nanoslips. When drop-cast from toluene solutions more concentrated than a few micromolar, molecular layers in which alkyl chains are more or less perpendicular to the surface were obtained, which may stack up into multilayer struc-

tures. This molecular layer can be a precursor to the nanoslips.

Electronic and optical properties of these ordered metal complex arrays are of great interest, with potential applications in molecule-based devices. In particular, these ordered arrays of highly luminescent species are suitable for investigation of electroluminescence or tunneling-current induced luminescence at the molecular level.[15–17]

Experimental Section

Syntheses—general: ^{1}H NMR spectra were recorded on a Jeol JNM-GX400 spectrometer. Mass spectrometers used were a Shimadzu GCMS-QP5050A spectrometer for EI-MS, an Applied Biosystems Voyager System 6123 for LDI-MS, and an Agilent G1969A spectrometer for CI-MS. Gas chromatography and gel permeation chromatography were conducted using a Shimadzu GC353B system with a TC-1 column and a Jai LC-9201 recycle GPC apparatus, respectively. EI-HRMS measurements were carried out by the Chemical Analysis Center of the College of Pharmacy, Nihon University. Elemental analyses were performed by the Chemical Analysis Center of the College of Science and Technology, Nihon University.

Iridium complexes, **Ir-C$_n$**, were prepared according to Scheme 1. The ligands with a long alkyl chain, 2-(3-alkoxyphenyl)pyridine, were obtained by alkylation of 3-iodophenol followed by the Stille coupling with 2-(tributylstannyl)pyridine.[18] Alternatively, the ligands could also be obtained by alkylation of 3-(pyridin-2-yl)phenol,[19] obtained by the Stille coupling of 3-iodophenol and 2-(tributylstannyl)pyridine.[18] The ligands thus prepared were refluxed in ethylene glycol with [Ir(acac)$_3$] to afford the desired **Ir-C$_n$**. Optical resolution ($>\approx 90\,\%$ *ee*) was achieved by chiral HPLC on a Jasco chromatograph (PU-1580) system equipped with a Chiralcel OD (Daicel) column by using hexane/2-propanol 96:4.

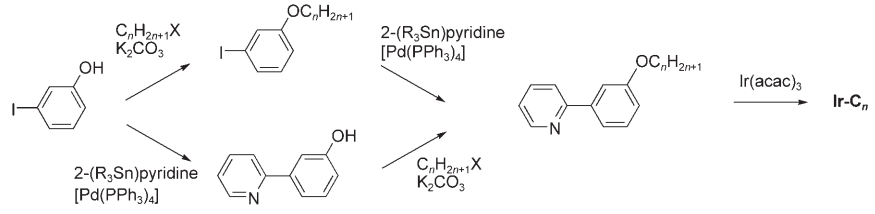

Scheme 1. Synthesis of **Ir-C$_n$**.

1-Docosyloxy-3-iodobenzene: A solution of 3-iodophenol (7.0 g, 32 mmol) and 1-bromodocosane (8.7 g, 22 mmol) in acetone (100 mL) was heated under reflux in the presence of K_2CO_3 (11.6 g) overnight. After the mixture was filtered, the solvent was evaporated, and the residue was redissolved in CH_2Cl_2. MeOH was added to the solution, and the solvent was mildly evaporated to remove CH_2Cl_2, resulting in the precipitation of a white solid (9.91 g, 83 %). ^{1}H NMR ($CDCl_3$): $\delta = 7.28$–7.23 (m, 2H; Ar2, Ar4), 6.98 (t, $J = 8.0$ Hz, 1H; Ar5), 6.85 (ddd, $J = 8.0$, 2.4, 0.8 Hz, 1H; Ar6), 3.91 (t, $J = 6.8$ Hz, 2H; OCH_2), 1.76 (quintet, $J = 6.8$ Hz, 2H; $OCCH_2$), 1.43 (quintet, $J = 6.8$ Hz, 2H; $OCCCH_2$), 1.4–1.2 (m, 36H; $(CH_2)_{18}$), 0.88 ppm (t, $J = 6.8$ Hz, 3H; CH_3); EI-HRMS: *m*/*z*: calcd for $C_{28}H_{49}IO$: 528.2828; found: 528.2828 $[M]^+$; purity (GC) $> 99.8\,\%$.

1-Iodo-3-octadecyloxybenzene: ^{1}H NMR ($CDCl_3$): $\delta = 7.23$–7.28 (m, 2H; H2, H6), 6.98 (t, $J = 8.0$ Hz, 1H; H5), 6.85 (ddd, $J = 8.0$, 2.4, 0.8 Hz, 1H; H4), 3.91 (t, $J = 6.8$ Hz, 2H; OCH_2), 1.76 (quintet, $J = 6.8$ Hz, 2H; $OCCH_2$), 1.43 (quintet, $J = 6.8$ Hz, 2H; $OCCCH_2$), 1.4–1.2 (m, 28H; $(CH_2)_{14}$), 0.88 ppm (t, $J = 6.8$ Hz, 3H; CH_3); CI-HRMS: *m*/*z*: calcd for $C_{24}H_{42}IO$: 473.2274; found: 473.2377 $[M+H]^+$.

2-(3-Docosyloxyphenyl)pyridine: A flask containing docosyloxy-3-iodobenzene (5.8 g, 11 mmol), 2-(tributylstannyl)pyridine (4.05 g, 11 mmol), and $[Pd(PPh_3)_4]$ (635 mg, 0.55 mmol) was evacuated in vacuum and then filled with N_2. Dry toluene (77 mL) deaerated with N_2 was introduced into the flask, and the mixture was heated under reflux overnight. After the mixture was filtrated, the solvent was evaporated, and the residue was purified by chromatography (silica gel, CH_2Cl_2) to afford a white solid (1.84 g, 35 %). ^{1}H NMR ($CDCl_3$): $\delta = 8.69$ (d, $J = 5.5$ Hz, 1H; py6), 7.74 (m, 2H; py3, py4), 7.56 (m, 1H; Ph2), 7.53 (d, $J = 8.0$ Hz, 1H; Ph6), 7.37 (t, $J = 8.0$ Hz, 1H; Ph5), 7.23 (m, 1H; py5), 6.96 (dd, $J = 8.0$, 2.4 Hz, 1H; Ph4), 4.05 (t, $J = 6.8$ Hz, 2H; OCH_2), 1.81 (quintet, $J = 6.8$ Hz, 2H; $OCCH_2$), 1.48 (quintet, $J = 6.8$ Hz, 2H; $OCCCH_2$), 1.4–1.2 (m, 36H; $(CH_2)_{18}$), 0.88 ppm (t, $J = 6.8$ Hz, 3H, CH_3); LDI-MS: *m*/*z*: 480 $[M+H]^+$; elemental analysis calcd (%) for $C_{33}H_{53}NO$: C 82.16, H 11.13, N 2.92; found: C 82.46, H 10.78, N 2.89.

2-(3-Octadecyloxyphenyl)pyridine: ^{1}H NMR ($CDCl_3$): $\delta = 8.69$ (d, $J = 5.5$ Hz, 1H; py6), 7.74 (m, 2H; py3, py4), 7.56 (m, 1H; Ph2), 7.53 (d, $J = 8.0$ Hz, 1H; Ph6), 7.37 (t, $J = 8.0$ Hz, 1H; Ph5), 7.23 (m, 1H; py5), 6.96 (dd, $J = 8.0$, 2.4 Hz, 1H; Ph4), 4.05 (t, $J = 6.8$ Hz, 2H; OCH_2), 1.81 (quintet, $J = 6.8$ Hz, 2H; $OCCH_2$), 1.48 (quintet, 6.8 Hz, 2H; $OCCCH_2$), 1.4–1.2 (m, 28H; $(CH_2)_{14}$), 0.88 ppm (t, $J = 6.8$ Hz, 3H; CH_3); EI-HRMS: *m*/*z*: calcd for $C_{29}H_{45}NO$: 423.3501; found: 423.3501 $[M]^+$; purity (GC) $= 100\,\%$.

2-(3-Triacontyloxyphenyl)pyridine: A mixture of 3-(pyridin-2-yl)phenol (55 mg, 0.32 mmol), 1-chlorotriacontane (100 mg, 0.22 mmol), and K_2CO_3 (400 mg, 2.89 mmol) in DMF was refluxed overnight. The reaction mixture was partitioned between CH_2Cl_2 and H_2O. The organic layer was taken, MeOH was added, and CH_2Cl_2 was mildly evaporated to precipitate out a white solid (174 mg). This crude material was used without further purification in the preparation of **Ir-C$_{30}$**. ^{1}H NMR ($CDCl_3$): $\delta = 8.69$ (d, $J = 5.5$ Hz, 1H; py6), 7.74 (m, 2H; py3, py4), 7.56 (m, 1H; Ph2), 7.53 (d, $J = 8.0$ Hz, 1H; Ph6), 7.37 (t, $J = 8.0$ Hz, 1H; Ph5), 7.23 (m, 1H; py5), 6.96 (dd, $J = 8.0$, 2.4 Hz, 1H; Ph4), 4.05 (t, $J = 6.8$ Hz, 2H; OCH_2), 1.81 (quintet, $J = 6.8$ Hz, 2H; $OCCH_2$), 1.48 (quintet, $J = 6.8$ Hz, 2H; $OCCCH_2$), 1.4–1.2 (m, 72H; $(CH_2)_{36}$), 0.88 ppm (t, $J = 6.8$ Hz, 3H; CH_3); LDI-MS: *m*/*z*: 591 $[M+H]^+$; EI-HRMS: *m*/*z*: calcd for $C_{41}H_{69}NO$: 591.5379; found: 591.5378 $[M]^+$; purity (GPC) $= 96\,\%$.

Ir-C$_{22}$: A mixture of 2-(3-decyloxyphenyl)pyridine (1.23 g, 2.6 mmol) and [Ir(acac)$_3$] (210 mg, 0.43 mmol) in ethylene glycol (4 mL) was heated under reflux under Ar for 4 d. MeOH was added to the reaction mixture to precipitate out the crude product, which was purified by chromatography (silica gel, CH_2Cl_2/hexane 1:1) to afford a yellow solid (246 mg, 35 %). ^{1}H NMR ($CDCl_3$): $\delta = 7.80$ (d, $J = 8.4$ Hz, 3H; py3), 7.56 (t, $J = 8.4$ Hz, 3H; py4), 7.52 (d, $J = 5.6$ Hz, 3H; py6), 7.23 (d, $J = 2.4$ Hz, 3H; Ph2), 6.83 (t, $J = 5.6$ Hz, 3H; py5), 6.62 (br, 3H; Ph5), 6.56 (dd, $J = 8.4$, 2.4 Hz, 3H; Ph4), 3.93 (t, $J = 6.8$ Hz, 6H; OCH_2), 1.74 (quintet, $J = 6.8$ Hz, 6H; $OCCH_2$), 1.43 (quintet, $J = 6.8$ Hz, 6H; $OCCCH_2$), 1.4–1.2 (m, 108H, $(CH_2)_{18}$), 0.88 ppm (t, $J = 6.8$ Hz, 9H; CH_3); CI-HRMS: *m*/*z*: calcd for $C_{99}H_{157}IrN_3O_3$: 1629.1860; found: 1629.1858 $[M+H]^+$; purity (GPC) $> 99\,\%$.

Ir-C$_{18}$: ^{1}H NMR ($CDCl_3$): $\delta = 7.80$ (d, $J = 8.4$ Hz, 3H; py3), 7.56 (t, $J = 8.4$ Hz, 3H; py4), 7.52 (d, $J = 5.6$ Hz, 3H; py6), 7.23 (d, $J = 2.4$ Hz, 3H; Ph2), 6.83 (t, $J = 5.8$ Hz, 3H; py5), 6.62 (br, 3H; Ph5), 6.56 (dd, $J = 8.4$, 2.4 Hz, 3H; Ph4), 3.93 (t, $J = 6.8$ Hz, 6H; OCH_2), 1.74 (quintet, $J = 6.8$ Hz, 6H; $OCCH_2$), 1.43 (quintet, $J = 6.8$ Hz, 6H; $OCCCH_2$), 1.4–1.2 (m, 84H; $(CH_2)_{14}$), 0.88 ppm (t, $J = 6.8$ Hz, 9H; CH_3); LDI-MS: *m*/*z*: 1460 $[M]^+$; elemental analysis calcd (%) for $C_{87}H_{132}IrN_3O_3$: C 71.56, H 9.11, N 2.88; found: C 71.40, H 8.85, N 2.72.

Ir-C_{30}: ^{1}H NMR ($CDCl_3$): $\delta = 7.80$ (d, $J = 8.4$ Hz, 3H; py3), 7.56 (t, $J = 8.4$ Hz, 3H; py4), 7.52 (d, $J = 5.6$ Hz, 3H; py6), 7.23 (d, $J = 2.4$ Hz, 3H; Ph2), 6.83 (t, $J = 5.6$ Hz, 3H; py5), 6.62 (br, 3H; Ph5), 6.56 (dd, $J = 8.4$, 2.4 Hz, 3H; Ph4), 3.93 (t, $J = 6.8$ Hz, 6H; OCH_2), 1.74 (quintet, $J = 6.8$ Hz, 6H; $OCCH_2$), 1.43 (quintet, $J = 6.8$ Hz, 6H; $OCCCH_2$), 1.4–1.2 (m, 216H; $(CH_2)_{36}$), 0.88 ppm (t, $J = 6.8$ Hz, 9H; CH_3); CI-HRMS: calcd for $C_{123}H_{205}IrN_3O_3$: 1965.5620; found: 1965.5556 $[M+H]^+$; purity (GPC) $> 99\,\%$.

Characterization of the assembly: STM-1 grade HOPG (12×12 mm) was purchased from GE Advanced Ceramics. STM and DFM measurements were carried out with an SII SPI3800N-SPA400 microscope under ambient conditions. Tips for STM measurements were made mechanically with Pt/Ir 9:1 wire. The bias voltages in Figure captions refer to the substrate voltage with respect to the tip. For the measurements at the liquid/solid interface, a droplet of an **Ir-C_n** solution in 1-phenyloctane was applied on the surface just below the tip using a syringe, after a freshly cleaved HOPG substrate was observed to confirm the atomic resolution of the tip. Samples to be observed at the air/solid interface were prepared by dropping a 4 μL toluene solution on the HOPG surface (12×12 mm), which was then air-dried. Annealing was carried out in an oven kept at a constant temperature (± 5 K) for an indicated duration, after which the temperature was lowered slowly at a rate of approximately 1 K min^{-1}. DFM (dynamic force microscopy or a dynamic force mode of atomic force microscopy) measurements were operated in a noncontact mode with an aluminum-coated silicon cantilever (SII SI-DF3) with a resonant frequency of 28–31 kHz, a tip radius of < 10 nm, and a spring constant of 1.7 N m^{-1}. Cyclic voltammetry was carried out with a Hokuto Denko HZ-3000 voltammetric analyzer for dried samples on HOPG, which was placed underneath an electrolyte solution (0.5 M Na_2SO_4 in H_2O). Pt and Ag wires were used as the counter and pseudoreference electrodes, respectively. IR-ERS spectra were measured on a Thermo Electron (Madison, WI) Nicolet 6700 FT-IR spectrometer equipped with a liquid nitrogen cooled mercury cadmium telluride detector with a modulation frequency of 60 kHz. The number of accumulations to improve the signal-to-noise ratio was 3000, and the spectral resolution was 4 cm^{-1}. The sample was vertically placed on a Harrick (Ossining, NY) VRA-1DG reflection attachment, which was set in the spectrometer. The *p*-polarized IR ray was generated by a Harrick PWG-U1R wire-grid polarizer. For the collection of background spectra, a cleaved surface of the HOPG block was used.

Acknowledgements

This work was partially supported by the Ministry of Education, Culture, Sports, Science and Technology, Japan (Grant-in-Aid for Scientific Research on Priority Areas, "Chemistry on Coordination Space" (18033050) and the High-Tech Research Center Project for Private Universities) and the Kurata Memorial Hitachi Science and Technology Foundation.

[1] a) D. L. Allara, *Nature* **2005**, *437*, 638–639; b) J. V. Barth, G. Costantini, K. Kern, *Nature* **2005**, *437*, 671–679.

[2] For reviews, see: a) D. M. Cyr, B. Venkataraman, ; G. W. Flynn, *Chem. Mater.* **1996**, *8*, 1600–1615; b) S. De Feyter, F. C. De Schryver, *Chem. Soc. Rev.* **2003**, *32*, 139–150; c) S. De Feyter, J. Hofkens, M. Van der Auweraer, R. J. M. Nolte, K. Müllen, F. C. Schryver, *Chem. Commun.* **2001**, 585–592; d) S. De Feyter, F. C. De Schryver, *J. Phys. Chem. B* **2005**, *109*, 4290–4302.

[3] a) X. Qiu, C. Wang, Q. Zeng, B. Xu, S. Yin, H. Wang, S. Xu, C. Bai, *J. Am. Chem. Soc.* **2000**, *122*, 5550–5556; b) X. Qiu, C. Wang, S. Yin, Q. Zeng, B. Xu, C. Bai, *J. Phys. Chem. B* **2000**, *104*, 3570–3574; c) H. Wang, C. Wang, Q. Zeng, S. Xu, S. Yin, B. Xu, C. Bai, *Surf. Interface Anal.* **2001**, *32*, 266–270.

[4] a) T. Ikeda, M. Asakawa, M. Goto, K. Miyake, T. Ishida, T. Shimizu, *Langmuir* **2004**, *20*, 5454–5459; b) J. Otsuki, E. Nagamine, T. Kondo, K. Iwasaki, M. Asakawa, K. Miyake, *J. Am. Chem. Soc.* **2005**, *127*, 10400–10405; c) J. Otsuki, S. Kawaguchi, T. Yamakawa, M. Asakawa, K. Miyake, *Langmuir* **2006**, *22*, 5708–5715.

[5] A few examples of metal complexes on HOPG have been observed by STM: a) L. Latterini, G. Pourtois, C. Moucheron, R. Lazzaroni, J.-L. Brédas, A. K.-D. Mesmaeker, F. C. De Schryver, *Chem. Eur. J.* **2000**, *6*, 1331–1336; b) D.-L. Shieh, K.-B. Shiu, J.-L. Lin, *Surf. Sci.* **2004**, *548*, L7–L12; c) J.-M. U. Ziener, J.-M. Lehn, A. Mourran, M. Möller, *Chem. Eur. J.* **2002**, *8*, 951–957; d) M. S. Alam, S. Strömsdörfer, V. Dremov, P. Müller, J. Kortus, M. Ruben, J.-M. Lehn, *Angew. Chem.* **2005**, *117*, 8109–8113; *Angew. Chem. Int. Ed.* **2005**, *44*, 7896–7900.

[6] a) M. A. Baldo, S. Lamansky, P. E. Burrows, M. E. Thompson, S. R. Forrest, *Appl. Phys. Lett.* **1999**, *75*, 4–6; b) C. Adachi, M. A. Baldo, S. R. Forrest, M. E. Thompson, *Appl. Phys. Lett.* **2000**, *77*, 904–906; c) G. He, O. Schneider, D. Qin, X. Zhou, M. Pfeiffer, K. Leo, *J. Appl. Phys.* **2004**, *95*, 5773–5777; d) K. Goushi, R. Kwong, J. J. Brown, H. Sasabe, C. Adachi, *J. Appl. Phys.* **2004**, *95*, 7798–7802.

[7] A. B. Tamayo, B. D. Alleyne, P. I. Djurovich, S. Lamansky, I. Tsyba, N. N. Ho, R. Bau, M. E. Thompson, *J. Am. Chem. Soc.* **2003**, *125*, 7377–7387.

[8] V. V. Grushin, N. Herron, D. D. LeCloux, W. J. Marshall, V. A. Petrov, Y. Wang, *Chem. Commun.* **2001**, 1494–1495.

[9] S. Yin, C. Wang, X. Qiu, B. Yu, C. Bai, *Surf. Interface Anal.* **2001**, *32*, 248–252.

[10] H. Onishi, A. Sasahara, H. Uetsuka, T. Ishibashi, *Appl. Surf. Sci.* **2002**, *188*, 257–264.

[11] R. G. Snyder, H. L. Strauss, C. A. Elliger, *J. Phys. Chem.* **1982**, *86*, 5145–5150.

[12] Y. Ohsawa, S. Sprouse, K. A. King, M. K. DeArmond, K. W. Hanck, R. J. Watts, *J. Phys. Chem.* **1987**, *91*, 1047–1054.

[13] a) L. C. Giancarlo, G. W. Flynn, *Acc. Chem. Res.* **2000**, *33*, 491–501; b) L. Pérez-García, D. B. Amabilino, *Chem. Soc. Rev.* **2002**, *31*, 342–356.

[14] We have observed a process of two-dimensional crystalline domain formation for a related tripod-type molecule: J. Otsuki, S. Shimizu, M. Fumino, *Langmuir* **2006**, *22*, 6056–6059.

[15] S. F. Alvarado, L. Rossi, P. Müller, P. F. Seidler, W. Riess, *IBM J. Res. Dev.* **2001**, *45*, 89–100.

[16] a) M. Vacha, Y. Koide, M. Kotani, H. Sato, *Chem. Phys. Lett.* **2004**, *388*, 263–268; b) M. Vacha, Y. Koide, M. Kotani, H. Sato, *J. Lumin.* **2004**, *107*, 51–56.

[17] Z.-C. Dong, A. S. Trifonov, X.-L. Guo, K. Amemiya, S. Yokoyama, T. Kamikado, T. Yamada, S. Mashiko, T. Okamato, *Surf. Sci.* **2003**, *532–535*, 237–243.

[18] M. van der Sluis, V. Beverwijk, A. Termaten, F. Bickelhaupt, H. Kooijman, A. L. Spek, *Organometallics* **1999**, *18*, 1402–1407.

[19] M. Terashima, K. Seki, C. Yoshida, K. Ohkura, Y. Kanaoka, *Chem. Pharm. Bull.* **1985**, *33*, 1009–1015.

Received: July 7, 2006
Published online: December 13, 2006

